Neutron capture of ^{46}Ca at thermonuclear energies

P. Mohr,[1,2] P. V. Sedyshev,[3] H. Beer,[4] W. Stadler,[2] H. Oberhummer,[2] Yu. P. Popov,[3] and W. Rochow[5]
[1]*Institut für Kernphysik, Technische Universität Darmstadt, Schlossgartenstrasse 9, D-64289 Darmstadt, Germany*
[2]*Institut für Kernphysik, Technische Universität Wien, Wiedner Hauptstrasse 8-10, A-1040 Vienna, Austria*
[3]*Frank Laboratory of Neutron Physics, JINR, 141980 Dubna, Moscow Region, Russia*
[4]*Forschungszentrum Karlsruhe, Institut für Kernphysik III, P. O. Box 3640, D-76021 Karlsruhe, Germany*
[5]*Physikalisches Institut, Universität Tübingen, Auf der Morgenstelle 14, D-72076 Tübingen, Germany*
(Received 19 January 1999)

The measurement of the neutron capture reaction ^{46}Ca$(n,\gamma)^{47}$Ca is of astrophysical interest, because ^{46}Ca is bypassed by charged-particle reactions. The nucleus ^{46}Ca is produced and destroyed by neutron-induced nucleosynthesis in hydrostatic helium, carbon, and neon burning through the reaction chain ^{45}Ca$(n,\gamma)^{46}$Ca$(n,\gamma)^{47}$Ca. At the Karlsruhe and Tübingen 3.75 MV Van de Graaff accelerators the thermonuclear ^{46}Ca$(n,\gamma)^{47}$Ca$(4.54\,d)$ cross section was measured by the activation technique via the 1297.09 keV γ-ray line of the ^{47}Ca decay. Samples of $CaCO_3$ enriched in ^{46}Ca by 5% were irradiated between two gold foils which served as capture standards using the ^{7}Li(p,n) and $T(p,n)$ reactions. The capture cross section was measured at the mean neutron energies 30, 104, 149, 180, and 215 keV, respectively. Maxwellian averaged capture cross sections were measured at the quasithermal neutron energies $kT=25$ and 52 keV, respectively. It was found that the ^{46}Ca$(n,\gamma)^{47}$Ca cross section in the thermonuclear energy region and at thermal energy is dominated by an *s*-wave resonance at 28.4 keV with a neutron width $\Gamma_n=(17.4^{+3.6}_{-2.8})$ keV and a radiation width $\Gamma_\gamma=(2.4\pm0.3)$ eV. The stellar reaction rate is determined in the temperature range from $kT=1$ to 250 keV and is compared with previous investigations using Hauser-Feshbach calculations or experimental cross section data. The astrophysical consequences of the new stellar reaction rate with respect to the nucleosynthetic abundance of ^{46}Ca are discussed. [S0556-2813(99)05106-7]

PACS number(s): 25.40.Lw, 25.40.Ny, 26.20.+f

I. INTRODUCTION

For a long time it has been known that the solar-system abundances of elements heavier than the iron-group nuclei have been produced by neutron-capture reactions [1]. However, neutron-induced reactions can also be of relevance for abundances of some isotopes lighter than the iron-group nuclei especially for neutron-rich isotopes, even though the bulk of these elements has been synthesized by charged-particle induced reactions. Examples for such neutron-rich isotopes that are bypassed by charged-particle reactions and produced by neutron-induced nucleosynthesis are ^{32}Si, ^{36}S, ^{40}Ar, and the calcium isotopes ^{46}Ca and ^{48}Ca [2–4].

^{46}Ca is one of the nuclei for which the largest nucleosynthetic abundance differences in model calculations can be obtained due to the use of varying reaction rates [4]. The isotope ^{46}Ca is an *s*-process nucleus produced in hydrostatic helium, carbon, and neon burning at temperatures of $0.2 \leqslant T_9 \leqslant 1.5$. The nucleosynthetic abundance of ^{46}Ca is determined by production and destruction through neutron capture in the reaction chain ^{45}Ca$(n,\gamma)^{46}$Ca$(n,\gamma)^{47}$Ca. The reaction rate for ^{46}Ca$(n,\gamma)^{47}$Ca has been determined previously using a Hauser-Feshbach calculation by Woosley *et al.* [5] (henceforth WHFZ). The reaction rate given by Thielemann *et al.* [6] (henceforth TAT) for ^{46}Ca$(n,\gamma)^{47}$Ca assumes a dominant *s*-wave behavior leading to a constant rate as a function of temperature. This constant rate was then normalized to the suggested experimental 30 keV (n,γ) cross section given in Ref. [7]. Finally, there exists the recent Hauser-Feshbach reaction rate calculated by Rauscher and Thielemann [8] (henceforth NON-SMOKER) including a modernized level density treatment and updated information on nuclear masses and energy levels as well as the option of treating isospin mixing.

The attempts to understand neutron-induced nucleosynthesis require as important ingredients the knowledge of neutron-capture rates. The influence of shell effects on neutron capture is one of the most interesting aspects of neutron capture, especially since neutron capture in the vicinity of magic numbers is often a bottleneck in neutron-induced nucleosynthesis. This is the case also in neutron capture on neutron-rich isotopes close to the magic proton and neutron numbers $Z=20$ and $N=28$, i.e., in the vicinity of the doubly magic nucleus ^{48}Ca. The neutron capture for nuclei in this mass region is also of relevance for the Ca-Ti abundance anomalies occurring in certain primitive meteorites [9–11].

The low isotopic occurrence of ^{46}Ca of only 0.004% in natural calcium which is only surpassed by the 0.00138% presence of ^{3}He in natural helium renders the study of the ^{46}Ca isotope difficult especially for time-of-flight neutron capture measurements. Neutron capture of ^{46}Ca$(n,\gamma)^{47}$Ca has been measured previously at thermal [12] and thermonuclear energies [13,14]. The results at thermonuclear energies are significantly different. The Maxwellian average capture cross section (MACS) at $kT=25$ keV of Käppeler *et al.* [13] is by a factor of 2.4 larger than the value reported by Murzin [14]. In addition, the values of Murzin suggest the existence of a broad resonance in ^{47}Ca at a neutron energy of 28 keV. In this work we tried to find evidence for this resonance and to resolve the discrepancy between the previous authors. For this purpose we carried out measurements at the Karlsruhe and Tübingen Van de Graaff accelerators. Quasi-

TABLE I. Sample characteristics and decay properties of the product nuclei ^{47}Ca and ^{198}Au.

Isotope	Chemical form	Isotopic composition (%)	Reaction	$T_{1/2}$ (d)	E_γ (keV)	Intensity per decay (%)
^{46}Ca	$CaCO_3$	81.363(40), 1.194(42), 0.385(43), 10.464(44), 4.987(46), 1.607(48)	^{46}Ca$(n,\gamma)^{47}$Ca	4.536	1297.09	74 ± 9 [a]
^{197}Au	metallic	100	^{197}Au$(n,\gamma)^{198}$Au	2.69	411.8047	95.50 ± 0.096

[a]From Ref. [25].

Maxwellian neutron spectra at $kT=25$ and 52 keV were generated as well as spectra very close to the ^{7}Li(p,n) reaction threshold with a mean energy of 30 keV. At energies above 100 keV we determined the ^{46}Ca capture cross section at average energies of 104, 149, 180, and 215 keV, respectively.

II. MEASUREMENTS

The activation measurements in the thermonuclear energy range have been carried out at the 3.75 MV Van de Graaff accelerators in Karlsruhe and Tübingen. Our activations were performed using samples with an enrichment of 5%. This was sufficient for the measurements due to the good signature for the ^{46}Ca capture events via the 1297 keV γ line in the 4.54 *d* decay of ^{47}Ca residual nucleus (Table I) and due to the good background conditions in activation experiments.

A. Activation technique

The activation technique has been described in previous publications [15–18]. The nuclei to be investigated are irradiated in the neutron spectrum provided by the Van de Graaff accelerator, and the induced activity is counted afterwards off-line in the laboratory via a characteristic γ line. The characteristic time constants of the activation are the irradiation time t_b, the counting time t_c, and the waiting time t_w. The γ-ray activity of the sample determined with a HPGe detector is given by

$$C=\epsilon_\gamma K_\gamma f_\gamma[1-\exp(-\lambda t_c)]\exp(-\lambda t_w)N\sigma_\gamma f_b\int_0^{t_b}\Phi(t)dt \tag{2.1}$$

with

$$f_b=\int_0^{t_b}\Phi(t)\exp(-\lambda t)dt \Big/ \int_0^{t_b}\Phi(t)dt.$$

The following additional quantities have been defined: ϵ_γ, Ge efficiency; K_γ, γ-ray absorption; f_γ, γ-ray intensity per decay; *N*, the thickness (atoms per barn) of target nuclei; σ_γ, the capture cross section; $\Phi(t)$, the neutron flux as a function of time. The quantity f_b is calculated from the registered flux history of a ^{6}Li glass monitor. Equation (2.1) contains the quantity σ_γ. The unknown capture cross section of ^{46}Ca is measured relative to the well-known standard cross section of ^{197}Au [19,20].

The efficiency determination of the 98.6% HPGe detector has been reported elsewhere [21]. The γ-ray absorption was calculated using tables published by Storm and Israel [22] and Veigele [23]. The samples of the $^{46}CaCO_3$ powder pressed to self-supporting tablets were heated to 1000 °C for 3 h. No measurable weight loss due to absorbed water was observed. The tablets were put into a thin Al-foil. The enrichment was determined by a mass spectrometric analysis carried out by the Wiederaufarbeitungsanlage Karlsruhe (WAK). In Table I the isotopic composition of the ^{46}Ca sample, other sample characteristics, and the decay properties of the product nuclei are listed. The decay of ^{47}Ca provided us with a strong γ-ray line at 1297.09 keV. Unfortunately, the intensity per decay is known only with a relative accuracy of 12%. It is interesting to note that in the two previous measurements [13,14] a γ-ray intensity of $(77\pm2)\%$ taken from [24] was used which in the new compilation [25] has been revised to $(74\pm9)\%$.

B. Neutron production, time-of-flight measurements

Two kinds of neutron spectra for the activations were generated, quasi-Maxwellian averaged distributions with thermal energies of $kT=25$ and 52 keV, respectively, using proton energies close to the reaction threshold of the ^{7}Li(p,n) and $T(p,n)$ reactions. For this purpose the target layer has to be chosen thick enough that the energy decrease of the protons reaches the reaction threshold in the layer. With these conditions we produced a kinematically collimated neutron beam which is independent from the target thickness. Using the ^{7}Li(p,n) reaction and proton energies very close to the threshold energy of 1881 keV we generated neutron spectra practically symmetrically centered around 30 keV but with neutron distributions between $20\leqslant E_n\leqslant 40$ keV and $12\leqslant E_n\leqslant 55$ keV, respectively (Fig. 1). With these spectra we were able to investigate the width of the ^{46}Ca *s*-wave resonance. The spectra at 104, 149, 180, and 214 keV were generated using 2.5 μm thick Li targets and higher proton energies.

The required proton energy conditions and the neutron spectra integrated over the solid angle of the sample were determined in time-of-flight (TOF) measurements before the actual activation runs using the accelerator in pulsed mode. The measurements were carried out under the same conditions as previously reported [18].

As the $^{46}CaCO_3$ samples of 6 mm diameter to be investigated are characterized by a finite thickness it is necessary to sandwich the sample by two comparatively thin gold foils of the same dimensions for the determination of the effective neutron flux at sample position. The activities of these gold foils were counted individually. The effective count rate of gold was obtained from these individual rates.

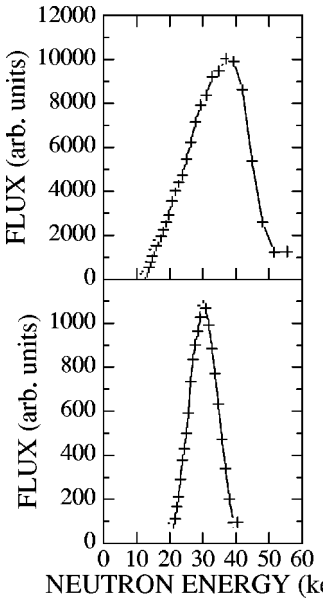

FIG. 1. The neutron spectra with a mean neutron energy of 30 keV generated at reaction threshold of the ^{7}Li(p,n) reaction. Below the distribution between $20 \leqslant E_n \leqslant 40$ keV and above the distribution between $12 \leqslant E_n \leqslant 55$ keV.

III. ANALYSIS

A. Experimental results

Table II gives a survey of the sample weights and the measured ^{46}Ca capture cross sections. The measurements were carried out with calcium carbonate sample masses between 60 and 80 mg. In Figs. 2 and 3 the accumulated γ-ray intensity from two of the ^{46}Ca activations is shown, the activation with a neutron spectrum of mean energy $kT=25$ keV and a mean energy 149 keV. In all γ-ray spectra the relevant γ line is well isolated on a low level of background counts.

The following systematic uncertainties were combined by quadratic error propagation, Au standard cross section: 1.5–3 %, Ge-detector efficiency: 2%, γ-ray intensity per decay: 12 % for the ^{47}Ca and 0.1 % for the ^{198}Au decay, divergence of neutron beam: 2–5 %, factor f_b: $\leqslant 0.5$ %, sample weight: <0.5 %.

B. Parameterization of the cross section

In the work of Murzin [14] average capture cross sections have been measured at the reactor with filtered neutron beams, the resolution of the energy spectra used lies between ± 0.5 and ± 12.5 keV (Fig. 4). His data suggest the existence of a broad s-wave resonance. With his data points from 17 eV to 45 keV and the thermal cross section of (0.74 ± 0.07) b [12] included he obtained for the resonance energy E_0 and the neutron and radiation widths Γ_n and Γ_γ the values (28.4 ± 1.6) keV, (17.7 ± 1.7) keV, and (1.4 ± 0.2) eV, respectively.

The existence of the 28 keV resonance is confirmed by our two measurements at energies around 30 keV. In general, the measured capture cross section is given by

$$\sigma_{\rm exp} = \int \Phi(E)\sigma(E)dE, \tag{3.1}$$

where $\Phi(E)$ is the normalized neutron energy distribution and $\sigma(E)$ is the capture cross section at the energy E. For a nonresonant cross section $\sigma(E)$ one would expect the same measured cross section $\sigma_{\rm exp}$ for the two neutron energy distributions at 30 ± 5 and 30 ± 10 keV (see Fig. 1). However, from the narrow energy distribution 30 ± 5 keV we obtain a cross section which is a factor of 1.5 larger than for the broader distribution 30 ± 10 keV. From this ratio of the two experimental results $\sigma_{\rm exp}$ at 30 keV one can directly derive the neutron width of the resonance using Eq. (3.1) with $\sigma(E)$ given by the Breit-Wigner formula

$$\sigma_{\rm BW}(E) = \frac{\pi}{k^2}\omega\frac{\Gamma_n\Gamma_\gamma}{(E-E_R)^2+\Gamma^2/4} \tag{3.2}$$

with the wave number k, the statistical factor $\omega=(2J+1)/[(2J_P+1)(2J_T+1)]=1$ for s-wave resonances, the resonance energy E_R, and the energy dependent widths Γ, Γ_n, and Γ_γ. For the neutron width at the resonance energy E_R we derive from our experimental data $\Gamma_n=(17.4^{+3.6}_{-2.8})$ keV. Obviously, such a broad resonance must be an s-wave resonance ($J^\pi=1/2^+$), and the energy dependence of the neutron width has to be taken into account. From the Breit-Wigner formula together with the experimental neutron width Γ_n we can additionally derive the radiation width of the resonance from our two measurements at (30 ± 5) and (30 ± 10) keV: $\Gamma_\gamma=(2.92 \pm 0.34)$ eV.

From the measurements using the quasithermal neutron spectra at $kT=25$ and 52 keV one can also derive the radiation width of the resonance. However, because of the broader energy distributions of the quasithermal spectra additional assumptions on the behavior of the capture cross section at higher energies enter into the determination. At higher energies an approximate $1/v$ behavior was found experimentally from the measurements at 104 ± 20, 149 ± 20, 180 ± 20, and 215 ± 23 keV. We have extrapolated this $1/v$ behavior down to lower energies until 44 keV where the resonant cross section exceeds the $1/v$ extrapolation neglecting interference effects (see Fig. 4). Note that the unphysical discontinuity above the 28.4 keV resonance at 44 keV has only minor influence on the astrophysical reaction rate, and that there is no discontinuity below the 28.4 keV resonance (see also Sec. III C). In the vicinity of the resonance we used a pure Breit-Wigner cross section. Again using Eq. (3.1) and a Maxwellian neutron energy distribution $\Phi(E)$ we obtain $\Gamma_\gamma=(1.88 \pm 0.33)$ eV from the MAC value at $kT=25$ keV and $\Gamma_\gamma=(2.4 \pm 1.0)$ eV from the MAC value at $kT=52$ keV. The weighted average of our three experimental Γ_γ values is (2.4 ± 0.3) eV. Our final resonance parameters for the s-wave resonance are then $E_0=28.4$ keV, $\Gamma_n=(17.4^{+3.6}_{-2.8})$ keV, and $\Gamma_\gamma=(2.4 \pm 0.3)$ eV.

The small discrepancy between the Γ_γ values can be partly caused by the uncertainty of the extrapolated $1/v$ cross section from the higher energy region. A better description of the higher energy region would require more detailed knowledge of the higher-lying resonances in ^{47}Ca above the ^{46}Ca$+n$ threshold which is not available.

TABLE II. Sample weights and experimental ^{46}Ca capture cross sections at thermonuclear energies.

Mean neutron energy (keV)	Mass of Au back side (mg)	Mass of $CaCO_3$ (mg)	Mass of Au front side (mg)	σ_γ (mb)	Uncertainty statistical (%)	Uncertainty total (%)
$kT=25$	16.620	75.298	16.630	4.807	0.32	13.0
	16.460	60.118	16.433	4.423	0.61	13.0
			Average	4.58 ± 0.59		
30 ± 5	15.665	75.298	15.530	14.537	2.5	13.7
	15.748	74.450	15.872	12.131	1.1	12.8
	15.967	77.767	15.976	13.034	1.1	12.8
	16.697	79.645	16.693	22.997	7.1	14.6
			Average	12.72 ± 1.62		
30 ± 10	16.183	77.767	16.177	6.536	0.91	13.0
	16.270	59.611	16.263	7.290	1.10	12.8
	16.005	76.079	15.930	10.317	0.91	12.8
	16.063	60.118	16.047	10.788	0.91	12.7
	16.127	75.728	16.230	7.929	0.80	12.8
	16.817	72.540	16.763	9.041	1.50	12.8
			Average	8.63 ± 1.10		
$kT=52$	16.270	59.611	16.263	3.13	19.70	23.8
			Average	3.13 ± 0.74		
104 ± 20	16.310	74.518	16.290	1.41	2.90	13.4
	16.627	76.079	16.647	1.63	0.90	13.6
			Average	1.52 ± 0.20		
149 ± 20	16.540	74.450	16.577	1.198	1.20	13.2
	16.867	76.079	16.853	1.173	2.10	13.3
			Average	1.19 ± 0.16		
180 ± 20	16.700	59.611	16.647	1.034	1.60	13.6
	16.130	74.450	15.997	1.073	1.50	13.8
			Average	1.05 ± 0.14		
215 ± 23	16.413	75.084	16.450	1.30	2.10	13.3
	16.670	75.298	16.663	0.92	5.20	14.1
			Average	1.11 ± 0.14		

C. The thermal capture cross section

Because of the known energy dependence of the neutron width Γ_n the thermal capture cross section can be calculated from the broad *s*-wave resonance using Eq. (3.2), and one obtains a thermal capture cross section of 1.315 b. This result is higher than the measured value from literature. However, one must keep in mind that destructive interference of this resonance capture with a direct *s*-wave capture component can reduce this thermal resonance capture. A simple estimate shows that a direct capture contribution of only 0.082 b is sufficient in order to obtain the experimental thermal value of (0.74 ± 0.07) b [12]. There is also some experimental evidence for the destructive interference between the broad resonance at the direct capture at low energies: Murzin's data point at 2 keV is lower than the 12 keV point, whereas the Breit-Wigner cross section is higher at 2 keV than at 12 keV.

D. Determination of the Maxwellian average capture cross section and the stellar rate factor

The obtained Maxwellian averaged ^{46}Ca$(n,\gamma)^{47}$Ca cross section determined from our experimental data including the measured MAC cross sections at $kT=25$ and 52 keV is shown by the solid line in Fig. 5. Our 30 keV experimental data served to determine the width of the *s*-wave resonance at 28.4 keV first suggested by Murzin. The experimental data above 100 keV were fitted assuming a $1/v$ energy dependence of the cross section. With the above parameters the MACS and the stellar rate factor were calculated and are given in Table III and shown in Figs. 5 and 6, respectively. In Table III we also show separately the contributions to the reaction rate factor for the *s*-wave resonance at 28.4 keV as well as for the $1/v$ part of the data above 44 keV where the

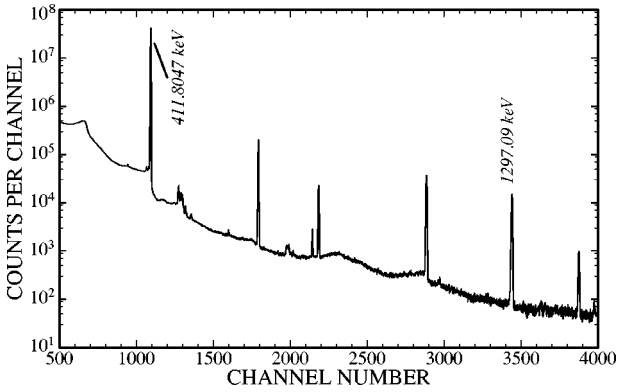

FIG. 2. Accumulated intensities of the ^{47}Ca and ^{198}Au γ-ray decay lines from the activation with the 75.298 mg $CaCO_3$ sample sandwiched by two Au foils using a neutron spectrum with a mean energy of $kT=25$ keV.

$1/v$ extrapolation from higher energies exceeds the resonant contribution from the 28 keV resonance.

The stellar rate factor can be fitted by the following analytic expression:

$$\langle \sigma v \rangle = \alpha_1 T_9^m \exp\left(-\frac{\alpha_2}{kT}\right) + \alpha_3 \exp\left(-\frac{E_R}{kT}\right). \qquad (3.3)$$

By fitting Eq. (3.3) to the obtained total stellar rate factor given in the last column of Table III we obtain the following set of parameters for the analytic fit: $\alpha_1=0.279 \times 10^6\,\mathrm{cm^3\,s^{-1}\,mole^{-1}}$, $\alpha_2=23.2$ keV, $\alpha_3=0.414 \times 10^6\,\mathrm{cm^3\,s^{-1}\,mole^{-1}}$, and $m=-1.395$. The analytic expression given in Eq. (3.3) with the above parameters reproduces the stellar rate factor for all temperatures by less than 1.3 % in the astrophysically interesting temperature range between $T=2\times10^8$ K and $T=2\times10^9$ K.

E. Comparison with previous results

As ^{46}Ca is very rare in nature (natural enrichment only 0.004%) it has not yet been investigated by the usual time-of-flight techniques. It is the advantage of the activation method that due to its high sensitivity and selectivity measurements are still possible with small samples of low enrichment, e.g., 5% as in our measurements. The results of previous ^{46}Ca neutron capture measurements in the thermonuclear energy region are also activation measurements but with discrepant results. To try to solve the discrepancies between these two measurements [13,14] represented one mo-

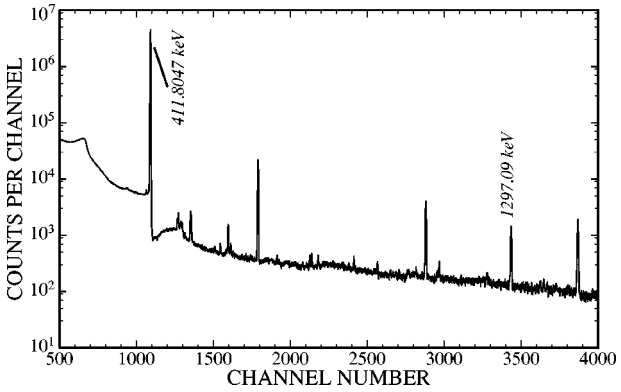

FIG. 3. Accumulated intensities of the ^{47}Ca and ^{198}Au γ-ray decay lines from the activation with the 74.450 mg $CaCO_3$ sample sandwiched by two Au foils using a neutron spectrum with a mean energy of 149 keV.

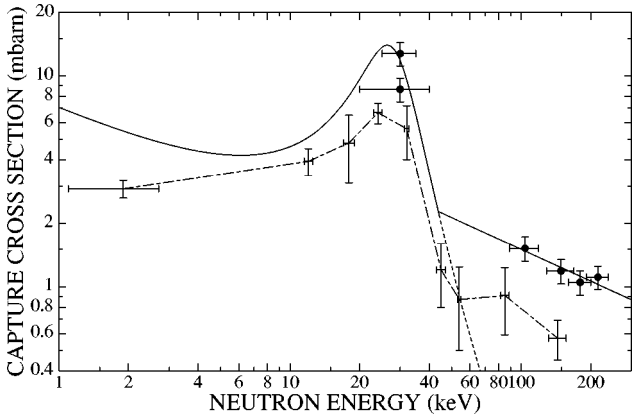

FIG. 4. Comparison of the experimental neutron capture cross section of ^{46}Ca with previous results. The data of Murzin [14] are connected by a dashed line as eyeguide. The values have been measured at the reactor with filtered neutron beams, the FWHM of the energy spectra lies between 1 and 25 keV, e.g., 144 ± 12.5 keV. The solid circles are the average cross sections of this work. The solid line is a determination of the ^{46}Ca capture cross section from our experimental data including the measured MAC cross sections at $kT=25$ and 52 keV, respectively. Our 30 keV average cross sections served to determine the width of the *s*-wave resonance at 28.4 keV first suggested by Murzin. The experimental data above 100 keV were fitted assuming a $1/v$ energy dependence of the cross section. The short-dashed line shows the contribution of the 28.4 keV resonance.

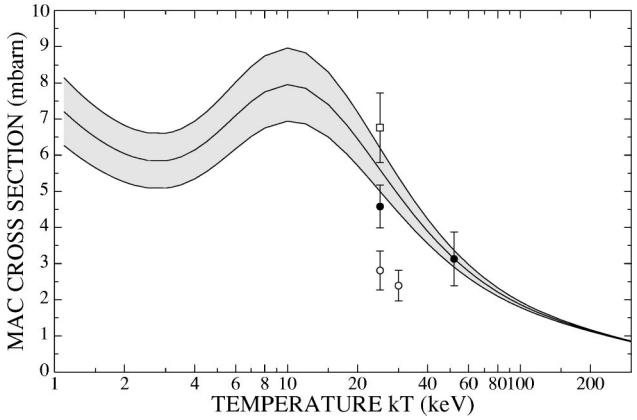

FIG. 5. A comparison of the experimental MAC cross sections from our measurements and from previous work is shown. The solid line with the shaded area represents the final MAC cross section and its 1σ uncertainty determined from all our measured capture cross sections. The two solid circles are our directly measured MAC cross sections at $kT=25$ and 52 keV. The open square is the MAC cross section measured by Käppeler *et al.* [13]. The open circles are the MAC cross sections at $kT=25$ and 30 keV reported by Murzin [14]. Note that the values from previous measurements have been corrected taking into account the change in the intensity per decay for the 1297 keV ^{47}Ca γ line from $I_\gamma=77\pm2\%$ to $I_\gamma=74\pm9\%$ [25].

TABLE III. The ^{46}Ca Maxwellian averaged capture (MAC) cross section and stellar reaction rate between 1 and 250 keV. The reaction rate contribution from the 28.4 keV resonance and the $1/v$ part above 44 keV are specified, too. The uncertainty is estimated to be 12.5%.

kT (keV)	$\langle\sigma v\rangle/v_T$ (mbarn)	Stellar rate factor $N_A\langle\sigma v\rangle$ ($cm^3mol^{-1}s^{-1}$)		
		Resonance part	$1/v$ part	Total
1.00	7.4609×10^{0}	1.9865×10^{5}	5.6428×10^{-13}	1.9865×10^{5}
2.00	6.0414×10^{0}	2.2748×10^{5}	9.3007×10^{-4}	2.2748×10^{5}
3.00	5.8470×10^{0}	2.6964×10^{5}	1.0142×10^{0}	2.6964×10^{5}
4.00	6.1427×10^{0}	3.2707×10^{5}	3.2258×10^{1}	3.2710×10^{5}
5.00	6.6225×10^{0}	3.9402×10^{5}	2.5167×10^{2}	3.9427×10^{5}
6.00	7.1002×10^{0}	4.6209×10^{5}	9.7656×10^{2}	4.6306×10^{5}
7.00	7.4856×10^{0}	5.2476×10^{5}	2.5482×10^{3}	5.2731×10^{5}
8.00	7.7510×10^{0}	5.7851×10^{5}	5.1960×10^{3}	5.8371×10^{5}
10.00	7.9543×10^{0}	6.5582×10^{5}	1.3905×10^{4}	6.6972×10^{5}
12.00	7.8485×10^{0}	6.9739×10^{5}	2.6496×10^{4}	7.2388×10^{5}
15.00	7.4000×10^{0}	7.1325×10^{5}	4.9828×10^{4}	7.6308×10^{5}
18.00	6.8346×10^{0}	6.9688×10^{5}	7.5163×10^{4}	7.7205×10^{5}
20.00	6.4556×10^{0}	6.7673×10^{5}	9.1952×10^{4}	7.6868×10^{5}
22.00	6.0939×10^{0}	6.5285×10^{5}	1.0818×10^{5}	7.6103×10^{5}
25.00	5.5970×10^{0}	6.1405×10^{5}	1.3105×10^{5}	7.4511×10^{5}
27.00	5.2984×10^{0}	5.8783×10^{5}	1.4519×10^{5}	7.3302×10^{5}
30.00	4.8975×10^{0}	5.4953×10^{5}	1.6468×10^{5}	7.1421×10^{5}
35.00	4.3400×10^{0}	4.9072×10^{5}	1.9290×10^{5}	6.8362×10^{5}
40.00	3.8942×10^{0}	4.3929×10^{5}	2.1646×10^{5}	6.5575×10^{5}
45.00	3.5337×10^{0}	3.9496×10^{5}	2.3618×10^{5}	6.3114×10^{5}
50.00	3.2383×10^{0}	3.5688×10^{5}	2.5280×10^{5}	6.0968×10^{5}
52.00	3.1349×10^{0}	3.4318×10^{5}	2.5871×10^{5}	6.0189×10^{5}
55.00	2.9930×10^{0}	3.2409×10^{5}	2.6691×10^{5}	5.9100×10^{5}
60.00	2.7867×10^{0}	2.9575×10^{5}	2.7897×10^{5}	5.7473×10^{5}
65.00	2.6111×10^{0}	2.7113×10^{5}	2.8938×10^{5}	5.6050×10^{5}
70.00	2.4601×10^{0}	2.4961×10^{5}	2.9841×10^{5}	5.4802×10^{5}
80.00	2.2141×10^{0}	2.1402×10^{5}	3.1324×10^{5}	5.2726×10^{5}
90.00	2.0223×10^{0}	1.8599×10^{5}	3.2482×10^{5}	5.1082×10^{5}
100.00	1.8687×10^{0}	1.6350×10^{5}	3.3403×10^{5}	4.9754×10^{5}
110.00	1.7426×10^{0}	1.4515×10^{5}	3.4144×10^{5}	4.8662×10^{5}
120.00	1.6371×10^{0}	1.2995×10^{5}	3.4746×10^{5}	4.7747×10^{5}
150.00	1.4008×10^{0}	9.7174×10^{4}	3.5940×10^{5}	4.5678×10^{5}
180.00	1.2357×10^{0}	7.6133×10^{4}	3.6478×10^{5}	4.4140×10^{5}
200.00	1.1483×10^{0}	6.5971×10^{4}	3.6568×10^{5}	4.3237×10^{5}
250.00	9.7616×10^{-1}	4.8479×10^{4}	3.6108×10^{5}	4.1095×10^{5}

tivation of the present experiment. In the approach of Käppeler *et al.* [13] a Maxwellian averaged capture cross section was measured directly at $kT=25$ keV using the quasi-Maxwellian neutron spectrum from the ^{7}Li(p,n) reaction. The measured MAC cross section at 25 keV was (6.5 ± 0.5) mb. In the work of Murzin [14] the Maxwellian average capture cross section has been calculated from values measured at the reactor with filtered neutron beams. This result was (2.7 ± 0.4) mb and turned out to be smaller by a factor of 2.4 than the respective MAC cross section value reported by Käppeler *et al.* [13] and induced Murzin to speculate about narrow *p*-wave resonances in the energy range missed in his measurement and therefore not taken into account in his calculation of the MAC cross section. In the present work we had used the methods of both previous investigations, i.e., neutron spectra which lead directly to MAC capture cross sections at $kT=25$ and 52 keV and neutron spectra to analyze the suggested *s*-wave resonance at 28.4 keV. Our average cross sections proved to be systematically higher than the results of Murzin [14] (Fig. 4). This tendency is also confirmed by our calculated MAC cross section of 5.6 ± 0.7 mb at $kT=25$ keV (taking into account all our experimental data as described in Secs. III B and III D) which is also higher than Murzin's [14] respective calculated result but slightly lower than Käppeler *et al.*'s [13] value (Fig. 5).

In Fig. 6 our new different stellar reaction rate factors are compared to previous results. The curves WHFZ and NONSMOKER refer to Hauser-Feshbach calculations given in Refs. [5,8], whereas for the TAT curve [6] a temperature-independent reaction rate factor is assumed that was normalized to the experimental MACS at 30 keV [7]. As can be

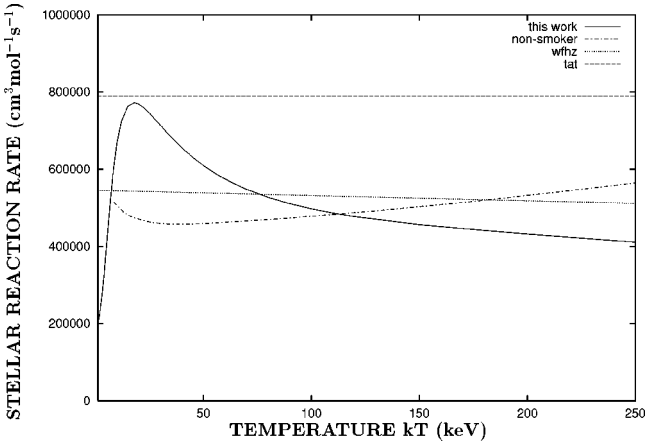

FIG. 6. A comparison of our new stellar reaction rate factor (solid curve) for ^{46}Ca$(n,\gamma)^{47}$Ca with previous determinations. The labels WHFZ (dotted curve) and NON-SMOKER (dash-dotted curve) refer to Hauser-Feshbach calculations, whereas for the TAT curve (dashed line) a temperature-independent reaction rate factor is assumed that was normalized to Käppeler's MACS at 30 keV.

seen from this figure, contrary to the previous determinations where there was no or only a small temperature dependence, our new reaction rate factor shows a much stronger temperature dependence. This is due to the effect of the *s*-wave resonance at 28.4 keV.

It is interesting that at the astrophysically relevant temperatures of $0.2 \leqslant T_9 \leqslant 1.5$ for hydrostatic helium, carbon, and neon burning the differences between the Hauser-Feshbach calculations WFHZ and NON-SMOKER and our new reaction rate factor are not large, even though the temperature dependence is quite different, e.g., at $T_9 = 1$, WFHZ: 5.3×10^5 cm^3 s^{-1} mole^{-1}; TAT: 7.9×10^5 cm^3 s^{-1} mole^{-1}; NON-SMOKER: 4.7×10^5 cm^3 s^{-1} mole^{-1}; this work: 5.2×10^5 cm^3 s^{-1} mole^{-1}. However, at lower or higher temperatures the differences get larger due to the stronger temperature dependence of our reaction rate factor.

The final stellar supernova yields for a 15 $M_\odot$ star evolved from the main sequence has been calculated in Ref. [4] using the WHFZ as well as the TAT rates. However, in this work the both the TAT rate and WFHZ rate for ^{46}Ca$(n,\gamma)^{47}$Ca have been normalized to the experimental MACS at 30 keV [7] giving a stellar reaction rate factor at $T_9 \approx 1$ of 7.9×10^5 and 7.8×10^5 cm^3 s^{-1} mole^{-1}, respectively. The difference calculated for the nucleosynthetic abundance of ^{46}Ca in Ref. [4] using the TAT and the WFHZ rates is practically only due to the production reaction rate ^{45}Ca$(n,\gamma)^{46}$Ca. Our new reaction rate factors for the reaction ^{46}Ca$(n,\gamma)^{47}$Ca leading to the destruction of ^{46}Ca is at $T_9 \approx 1$ about a factor 1.5 smaller than the one used in Ref. [4]. This leads to an enhancement of the nucleosynthetic abundance of ^{46}Ca for our new stellar reaction rate factor by about the same amount.

IV. CONCLUSIONS

The ^{46}Ca neutron capture cross section in the thermonuclear energy region is dominated by a *s*-wave resonance at 28.4 keV. The thermal capture cross section is due to this resonance chiefly resonance capture, too. Only a very small direct contribution of 0.082 b is sufficient to generate by destructive interference the measured thermal capture cross section. For further investigations it would be of great importance to measure the intensity per decay I_γ of the 1297 keV γ-ray line in the ^{47}Ca decay to a higher precision. The 12% relative uncertainty of I_γ is presently the dominating uncertainty in the measurements.

Our new reaction rate factor for ^{46}Ca$(n,\gamma)^{47}$Ca shows, contrary to previous determinations, a much stronger temperature dependence due to a resonant *s*-wave contribution. Furthermore, it is smaller than previous determinations of the reaction rate that have been normalized to the experimental Maxwellian cross section at 30 keV [7]. This leads to an enhanced nucleosynthetic abundance of ^{46}Ca by about a factor 1.5 compared to the values given in Ref. [4].

ACKNOWLEDGMENTS

We thank to A. Murzin for his cooperation in providing us with the ^{46}Ca results of his Ph.D. thesis. The interest and support of Professor G. J. Wagner, Universität Tübingen, and the provision of a 100% HPGe detector from Institut für Strahlenphysik, Universität Stuttgart, for the experiment is gratefully acknowledged. We would like to thank the technicians of the Van de Graaff accelerators, G. Rupp and M. Brandt, and the Karlsruhe Van de Graaff staff members E.P. Knaetsch, D. Roller, and W. Seith for their help and support of the experiment especially in the preparation of the metallic Li targets. We are grateful to T. Rauscher for providing the NON-SMOKER reaction rates from his reaction library. We thank the Fonds zur Förderung der wissenschaftlichen Forschung in Österreich (Project No. S7307-AST), the Deutsche Forschungsgemeinschaft (DFG) (Project No. Mo739/1-1), and Volkswagen-Stiftung (No. Az: I/72286) for their support.

[1] E. M. Burbidge, G. R. Burbidge, W. A. Fowler, and F. Hoyle, Rev. Mod. Phys. **29**, 547 (1957).

[2] H. Beer and R.-D. Penzhorn, Astron. Astrophys. **174**, 323 (1987).

[3] H. Schatz, S. Jaag, G. Linker, R. Steininger, F. Käppeler, P. E. Koehler, S. M. Graff, and M. Wiescher, Phys. Rev. C **51**, 379 (1995).

[4] R. D. Hoffman, S. E. Woosley, T. A. Weaver, T. Rauscher, and F.-K. Thielemann, astro-ph/9809240.

[5] S. E. Woosley, W. A. Fowler, J. A. Holmes, and B. A. Zimmermann, At. Data Nucl. Data Tables **22**, 371 (1978).

[6] F.-K. Thielemann, M. Arnould, and J. Truran, in *Advances in Nuclear Astrophysics*, edited by E. Vangioni-Flam (Editions Fronitière, Gif sur Yvette, 1987), p. 525.

[7] Z. Y. Bao and F. Käppeler, At. Data Nucl. Data Tables **36**, 411 (1987).

[8] T. Rauscher and F.-K. Thielemann, in *Stellar Evolution, Stellar Explosions, and Galactic Chemical Evolution*, edited by A.

Mezzacappa (IOP, Bristol, 1998), p. 519; T. Rauscher, NONSMOKER library (unpublished), URL http://quasar.physik.unibas.ch/~tommy/reaclib.html#non-smoker
[9] D. G. Sandler, S. E. Koonin, and W. A. Fowler, Astrophys. J. **259**, 908 (1982).
[10] W. Ziegert *et al.*, Phys. Rev. Lett. **55**, 1935 (1985).
[11] A. Wöhr *et al.*, in *Proceedings of the Eighth International Symposium on Gamma-Ray Spectroscopy and Related Topics, 20.-24.9. 1993*, Fribourg, Switzerland, edited by J. Kern (World Scientific, Singapore, 1994), p. 762.
[12] S. F. Mughabghab, M. Divadeenam, and N. E. Holden, *Neutron Cross Sections* (Academic Press, New York, 1981), Vol. I.
[13] F. Käppeler, G. Walter, and G. J. Mathews, Astrophys. J. **291**, 319 (1985).
[14] A. Murzin, Ph.D. thesis, Institute for Nuclear Research of Ukrainian Academy of Sciences, Kiev, 1993.
[15] H. Beer and F. Käppeler, Phys. Rev. C **21**, 534 (1980).
[16] F. Käppeler, A. A. Naqvi, and M. Al-Ohali, Phys. Rev. C **35**, 936 (1987).
[17] H. Beer, G. Rupp, F. Voß, and F. Käppeler, Nucl. Instrum. Methods Phys. Res. A **337**, 492 (1994).
[18] H. Beer, P. V. Sedyshev, Yu. P. Popov, W. Balogh, H. Herndl, and H. Oberhummer, Phys. Rev. C **52**, 3442 (1995).
[19] R. L. Macklin (private communication).
[20] W. Ratynski and F. Käppeler, Phys. Rev. C **37**, 595 (1988).
[21] P. Mohr, H. Oberhummer, H. Beer, W. Rochow, V. Kölle, G. Staudt, P. V. Sedyshev, and Yu. P. Popov, Phys. Rev. C **56**, 1154 (1997).
[22] E. Storm and H. Israel, Nucl. Data, Sect. A **7**, 565 (1970).
[23] W. J. Veigele, At. Data Nucl. Data Tables **5**, 51 (1973).
[24] C. M. Lederer and V. S. Shirley, *Table of Isotopes*, 7th ed. (Wiley, New York, 1978), p. 122.
[25] R. B. Firestone and V. S. Shirley, *Table of Isotopes*, 8th ed. (Wiley, New York, 1996), Vol. I, p. 175.